Volume 3 | Number 8 | August 2019

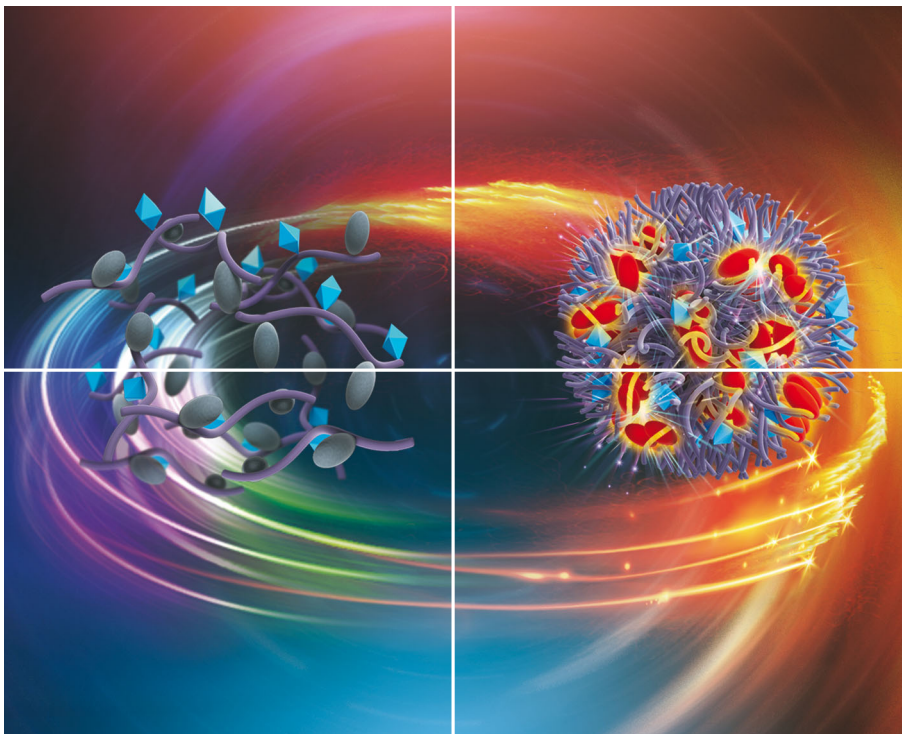

MATERIALS CHEMISTRY

FRONTIERS

CCS 中国化学会 CHINESE CHEMICAL SOCIETY
ICCAS 1956
ROYAL SOCIETY OF CHEMISTRY | Celebrating IYPT 2019
rsc.li/frontiers-materials

MATERIALS CHEMISTRY
FRONTIERS

RESEARCH ARTICLE

View Article Online
View Journal | View Issue

Cite this: *Mater. Chem. Front.*, 2019, **3**, 1503

Fluorescent thermometer based on a quinolinemalononitrile copolymer with aggregation-induced emission characteristics†

Jinfeng Yang,[ab] Kaizhi Gu,[a] Chuanxing Shi,[a] Meng Li,[c] Ping Zhao*[a] and Wei-Hong Zhu *[a]

Received 11th March 2019,
Accepted 28th March 2019

DOI: 10.1039/c9qm00147f

rsc.li/frontiers-materials

Fluorescent molecular thermometers are of great importance because of their potential biomedical applications. However, conventional fluorescent thermometers always face the serious problem of thermal-induced fluorescence quenching. Given that the fluorescence behavior of aggregation-induced emission luminogen (AIEgen)-containing polymers still needs improvement, here we report an AIEgen-grafted copolymer **P(NIPAM-*co*-EM)** with a thermo-responsive polymer poly(*N*-isopropyl acrylamide) (**PNIPAM**) as a matrix for constructing an AIE fluorescent thermometer. Considering the thermal and fluorescence behaviors, the aqueous copolymer exhibits a specific lower critical solution temperature (LCST) at about 30 °C, along with a fluorescence enhancement of 3.1-fold during the phase transition from 30 to 45 °C. Significantly, the temperature-dependent photophysical characteristic reveals that the fluorescence signal of **P(NIPAM-*co*-EM)** can be switched reversibly, thereby achieving the nondestructive sensing of temperature. The resulting copolymer **P(NIPAM-*co*-EM)** shows an interesting aggregation-induced enhanced emission (AIEE) activity, which is attributed to the grafted AIE-active unit of quinolinemalononitrile tangled with polymer chains. As demonstrated, the AIEgen-grafted copolymer can be potentially developed as a fluorescent thermometer through its AIEE mechanism.

Introduction

Fluorescent chemosensors have become a growing interest due to their broad applications in diverse fields, such as biology, pharmacology, and environmental sciences.[1–8] However, the traditional chromophores always suffer from the thorny aggregation-caused quenching (ACQ) effect.[9–12] It is highly desirable to develop fluorophores with solid-state emission to avoid the troublesome ACQ limitation. Tang's group have observed the intriguing solid-state enhanced emission phenomenon, that is, aggregation-induced emission (AIE) or aggregation-induced enhanced emission (AIEE).[13–17] Recently, AIE luminogens (AIEgens) have received more attention in materials science, especially in achieving on-site sensing and long-term cell tracking.[18–25] It is well understood that the restriction of intramolecular motion (RIM) is considered to be the predominant reason for the AIE phenomenon, in which the nonradiative channel *via* the rotational/vibrational energy relaxation process can be well suppressed in the aggregation or at higher viscosity, thereby leading to the efficient radiative decay of excited states.[14] However, the fluorescence behavior of AIEgen-containing polymers still needs improvement.

Optical thermometers are of great importance because of their technological significance and potential biomedical applications.[26–30] At high temperature, biopolymers can undergo conformation changes, and lead to protein aggregation or fibrillogenesis. Many biological events often vary with body temperature, like ATP hydrolysis or hyperpyrexia.[31,32] Poly(*N*-isopropylacrylamide) (**PNIPAM**) is a well-known thermo-responsive polymer with a characterized phase transition temperature designated as the lower critical solution temperature (LCST) at about 30 °C.[33] Specifically, **PNIPAM** exhibits a polar character at low temperature (coil colloid), but a rise in temperature results in the formation of a less polar domain inside the polymer chain associated with the polymeric globular aggregation.[34,35] Given its specific biocompatibility and phase transition properties with

[a] *Shanghai Key Laboratory of Functional Materials Chemistry, Key Laboratory for Advanced Materials and Institute of Fine Chemicals, Joint International Research Laboratory of Precision Chemistry and Molecular Engineering, Feringa Nobel Prize Scientist Joint Research Center, School of Chemistry and Molecular Engineering, East China University of Science & Technology, Shanghai 200237, China. E-mail: whzhu@ecust.edu.cn, pzhao@ecust.edu.cn*
[b] *School of Chemistry and Chemical Engineering, Key Laboratory for Green Processing of Chemical Engineering of Xinjiang Bingtuan, Shihezi University, North 4th Road, Shihezi, Xinjiang 832003, China*
[c] *Department of Environmental Science and Engineering, North China Electric Power University, Baoding 071003, China*

† Electronic supplementary information (ESI) available. CCDC 1902267. For ESI and crystallographic data in CIF or other electronic format see DOI: 10.1039/c9qm00147f

temperature, **PNIPAM** is expected to be a good matrix to graft a fluorescent chromophore for constructing a fluorescent thermometer.[36–39] However, the conventional fluorescent thermometers always face the serious problem of thermal-induced fluorescence quenching due to the fierce thermal vibration or the formation of globular aggregates, leading to strong π–π stacking.[40] Therefore, the AIEgen-grafted **PNIPAM** might be an ideal candidate for developing a thermal- or environment-sensitive system.

Much effort has been expended toward the discovery of organic or polymeric AIE systems, mostly focusing on silole, coumarin–pyrazole hybrid, tetraphenylethene and cyanostilbene derivatives.[13,41–44] Given that many near-infrared chromophores have a characteristic donor–π–acceptor (D–π–A) feature,[45,46] like the red-emitting AIEgen of quinolinemalononitrile,[21,47–52] here we report an AIEgen-grafted copolymer **P(NIPAM-*co*-EM)** for constructing a fluorescent thermometer (Scheme 1), in which the quinolinemalononitrile-based AIEgen is incorporated into thermo-responsive **PNIPAM**. The main principle is that the temperature effect on the microstructure of the **PNIPAM** chain can directly promote the aggregation behavior of the grafted AIEgen, thereby achieving a specific AIE-active fluorescent thermometer.

Results and discussion

Synthesis and characterization

Generally, a fluorescent thermometer should consist of a thermo-sensitive moiety and a fluorescent reporting unit. In this study, the as-prepared fluorescent thermometer **P(NIPAM-*co*-EM)** is composed of **NIPAM** and a quinolinemalononitrile-based AIEgen, which are utilized as the thermo-responsive and signal reporting unit, respectively, and its synthetic route is depicted in Scheme 1. Firstly, intermediate **2** was obtained through Knoevenagel reaction between 4-(piperazin-1-yl)benzaldehyde with quinolinemalononitrile AIEgen (**1**), and further functionalized with methacryloyl chloride to obtain the corresponding AIEgen monomer **EM**. Finally, the targeted fluorescent thermometer **P(NIPAM-*co*-EM)** was prepared by the radical polymerization of the AIEgen monomer **EM** and thermo-responsive monomer **NIPAM**.

In the ^{1}H NMR spectrum of the AIEgen monomer **EM**, the characteristic coupling constant (J = 16.0 Hz) of alkene hydrogen protons is indicative of the predominant *trans*-configuration (Fig. S1, ESI†). For **P(NIPAM-*co*-EM)**, the protons of aromatic rings are located at the range of 6.9–7.7 ppm, revealing that the AIEgen monomer **EM** is successfully decorated onto the **PNIPAM** chain through the simple radical polymerization (Fig. 1A). Moreover, according to the corresponding integral area of hydrogen in the ^{1}H NMR spectrum, the molar ratio of **EM** and **NIPAM** units in the copolymer composition was about 1 : 291. Meanwhile, we also investigated the molar ratio by the standard working curve of absorption spectra in tetrahydrofuran (THF) solution. Based on the Lambert–Beer law and conservation of mass, we determined that the monomer molar ratio of the **EM** and **NIPAM** units is about 1 : 226 (Fig. 1B–D), which is very close to the result obtained from the ^{1}H NMR spectrum. With polystyrene as a standard, the GPC-determined number-average molecular weight (M_n) of **P(NIPAM-*co*-EM)** is 6956, and polydispersity (M_w/M_n) is 1.61 (Fig. S2, ESI†), indicating that the copolymer shows a narrow molecular weight distribution.

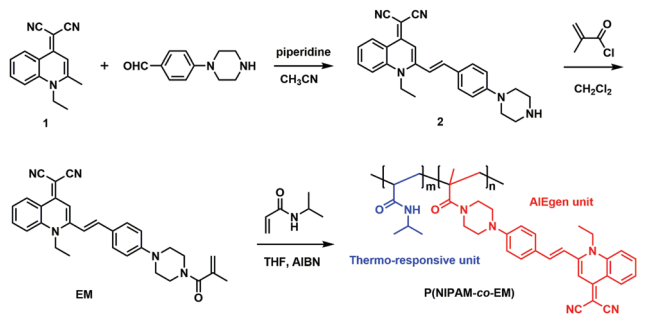

Scheme 1 Synthetic route of the fluorescent thermometer **P(NIPAM-*co*-EM)** containing the side-chain grafted AIEgen of quinolinemalononitrile.

AIE properties of monomer EM

THF is a good solvent for dissolving **EM**, while water is a poor solvent. It is expected that increasing the water fraction (f_w) in the THF/H_2O mixtures can lead to the aggregation of **EM**. As shown in Fig. 2A, the absorption spectra of **EM** were slightly affected even if the f_w was increased up to 70%. However, upon increasing the f_w to 80–90%, the absorption intensity dropped dramatically with a long tail due to the molecular aggregation. As shown in Fig. 2B, the monomer of **EM** showed very weak fluorescence with a peak at 587 nm, a typical orange emission (inset of Fig. 2B). During the f_w increase to 70%, the emission intensity of **EM** was enhanced with a slight red-shift from 587 to 601 nm. The observed continuous emission enhancement and red-shift by about 14 nm might arise from the concerted effect of the water polarity and the resultant formation of the J-aggregate nanoparticles.[52] Successively, the emission intensity was still enhanced but with a small blue-shift when the water fraction was up to 90%, which can be possibly attributed to the possible formation of amorphous aggregates with random but tight stacking structure.[51,52] As shown in the scanning electron microscopy (SEM) images of **EM** prepared by the THF/H_2O mixtures (f_w = 90%), we clearly found the resulting nanoparticles with a diameter of about 200–300 nm (Fig. 2C). Notably, the powder of the AIEgen monomer **EM** exhibited strong orange emission (Fig. 2D), indicative of a typical AIE behavior.

Crystal structure of the AIEgen monomer EM with distorted *trans*-configuration

For further insight into the aggregation behavior, the mixture solvent of dichloromethane/*n*-hexane (1 : 1, v/v) was diffused to obtain the single crystal of the AIEgen monomer **EM** (Table S1, ESI†). As illustrated in Fig. 3A, **EM** adopts the distorted *trans*-configuration, in which the twisted angles of the ethylene double bond with the quinoline and benzene ring are 36.0° and 19.0°, respectively. Obviously, the twisted molecular configuration can effectively prevent the molecules from π···π stacking, which is conducive to the solid fluorescence emission.

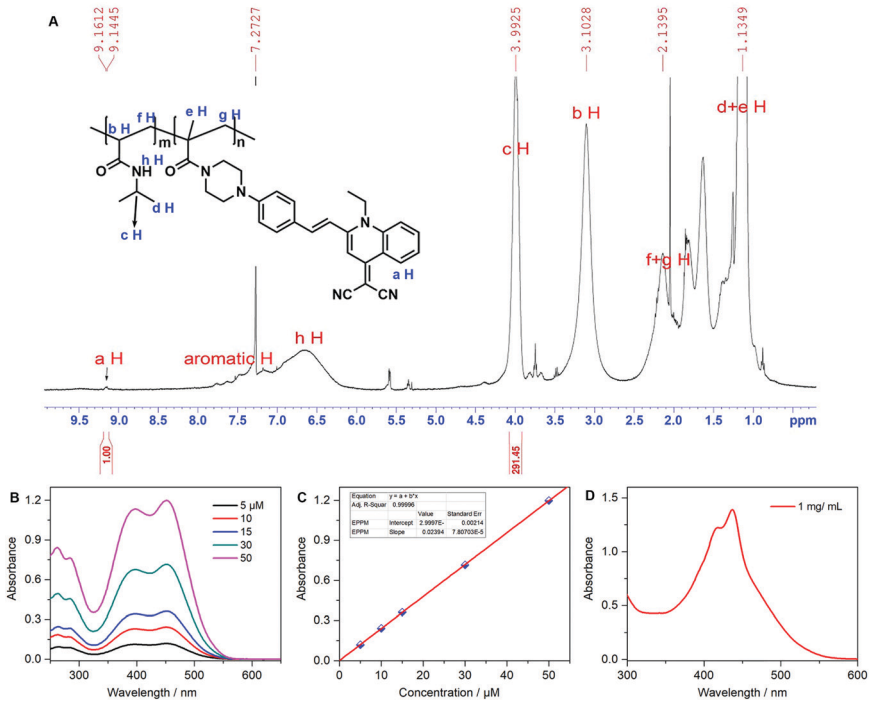

Fig. 1 Structure characterization of the fluorescent thermometer system: (A) ^{1}H NMR spectra of copolymer **P(NIPAM-*co*-EM)** in $CDCl_3$. (B) Absorption spectra of the AIEgen monomer **EM** at different concentrations in THF (5–50 μM). (C) The corresponding standard working curve obtained from absorbance at 452 nm as a function of concentration. (D) Absorption spectrum of **P(NIPAM-*co*-EM)** in THF (1.0 mg mL^{-1}).

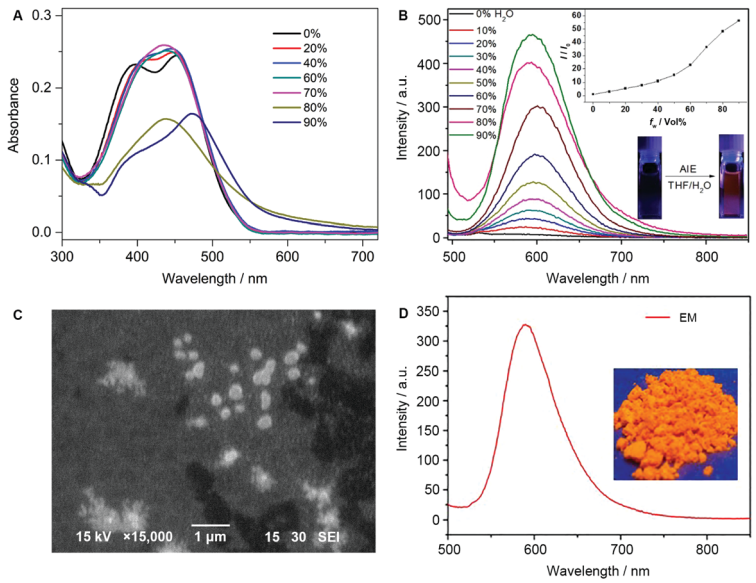

Fig. 2 Absorption and emission spectra: (A) absorption and (B) emission spectra of the AIEgen monomer **EM** (10 μM) in H_2O/THF mixtures with different water fraction (f_w) from 0–90%, λ_{ex} = 460 nm; insets (B): plot of relative emission intensity against f_w and fluorescent images of **EM** (f_w = 0 and 90%) under UV light illumination. (C) SEM image of nanoaggregates obtained from the **EM** suspension (f_w = 90%). (D) Emission spectrum of **EM** in the solid state, λ_{ex} = 460 nm; inset: fluorescent image of the solid **EM** under UV light illumination.

The molecular accumulation topology showed that the chemical structure of **EM** appears at the high molecular distortion (Fig. 3B), which does not have π···π stacking belonging to the face-to-face interactions from an aromatic ring. Through the intermolecular weak CH···N (2.643 Å) and CH···π (2.795 Å) hydrogen bonds, the tight packing of the **EM** molecules can effectively restrict the intramolecular rotation and intermolecular vibrations, and thus realize the specific AIE behavior, that is, making **EM** produce high solid fluorescence (Fig. 2D).

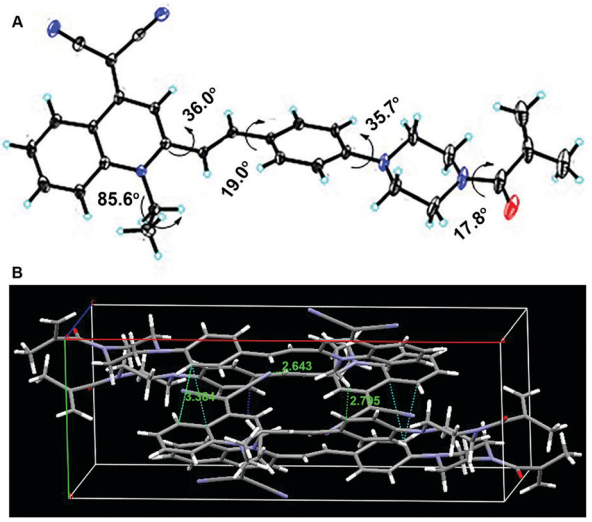

Fig. 3 Crystal structure of the AIEgen monomer **EM**: (A) X-ray single-crystal structure and (B) molecular stacking diagram of **EM**.

AIEE properties of copolymer P(NIPAM-*co*-EM)

The measurements of the emission spectra for **P(NIPAM-*co*-EM)** in THF and THF/H_2O were conducted to determine the polymeric fluorescence behavior. As shown in Fig. 4A, the absorption spectra also indicated that the absorbance increases a little with a blue-shift, which might result from the possible existence of the micelle nanoparticles. As shown in Fig. 4B, the linear polymer was emissive in the THF solution (15.6 μM) to some extent, and the fluorescence decreased a little upon adding 10% water, due to the twisted intramolecular charge transfer process resulting from the D–π–A featuring **EM** unit. In contrast with higher water fraction, the fluorescence started to increase continuously with a 3.1-fold enhancement factor, attributed to the formation of the micelle nanoparticles. In the system of **P(NIPAM-*co*-EM)**, the side-chain grafted AIEgen units of **EM** are entangled with polymer chains, which can restrict their intramolecular rotation to some extent and thus render the polymer somewhat emissive in the solution state. This behavior is different from the luminous characteristic of the monomer **EM**. However, there was a sharp increase when the water fraction reached 90%. Moreover, the concentration effect on the photophysical property was also examined. At a higher concentration of 38.4 μM, **P(NIPAM-*co*-EPPM)** still showed a fluorescence enhancement with higher water fraction (Fig. S3, ESI†). Indeed, **P(NIPAM-*co*-EM)** shows a typical AIEE effect, along with achieving the strong orange emission in the solid powder state (Fig. S4, ESI†).

Fluorescence quantum efficiency

To evaluate the emissions quantitatively, the quantum efficiencies of monomer **EM** or **P(NIPAM-*co*-EM)** in dilute solution ($\Phi_{F,s}$), in thin film ($\Phi_{F,f}$), in the solid powder ($\Phi_{F,p}$) and in aggregation states ($\Phi_{F,a}$) were further studied. For the monomer **EM**, the fluorescence quantum yield (Φ_F) exhibited an enhancement factor ($\alpha_{AIE} = \Phi_{F,a}/\Phi_{F,s}$) of 56-fold from the pure THF solution to the mixed THF/water (f_w = 90%) solution. And, the fluorescence quantum yield of the solid

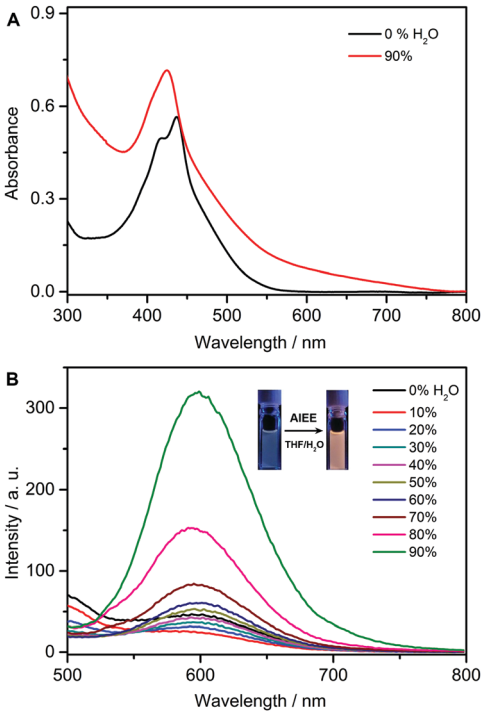

Fig. 4 AIEE behavior of the copolymer. (A) Absorption and (B) emission spectra of copolymer **P(NIPAM-*co*-EM)** (15.6 μM) in H_2O/THF mixtures with different f_w, λ_{ex} = 430 nm; inset (B): fluorescence images of the **P(NIPAM-*co*-EM)** (f_w = 0 and 90%) under UV light irradiation.

Table 1 Optical properties and fluorescence quantum efficiency of **EM** and **P(NIPAM-*co*-EM)**

	λ_{abs}/nm	λ_{em}/nm			
Emitters	Soln[a]	Soln ($\Phi_{F,s}$)[b]	Aggr ($\Phi_{F,a}$)[b]	Film ($\Phi_{F,f}$)[c]	Powder ($\Phi_{F,p}$)[c]
EM	450	587 (0.1)	594 (5.6)	615 (2.6)	590 (4.2)
P(NIPAM-*co*-EM)	437	595 (1.4)	597 (4.4)	610 (5.5)	600 (5.9)

[a] Abbreviation: soln = solution (10 μM in THF), aggr = THF/water mixtures with 90% water fraction, film = prepared through drop casting of dichloromethane solution, λ_{abs} = absorption maximum, λ_{em} = emission maximum, and Φ_F = fluorescence quantum yield. [b] Estimated using rhodamine B as standard (Φ_F = 50% in ethanol), at the optical density of the solution lower than 0.05 for avoiding self-absorption. [c] Measured by integrating sphere.

powder and film for **EM** was determined to be 4.2% and 2.6% (Table 1), respectively. Notably, the $\Phi_{F,s}$, $\Phi_{F,a}$, $\Phi_{F,f}$ and $\Phi_{F,p}$ values of **P(NIPAM-*co*-EM)** were 1.4%, 4.4%, 5.5% and 5.9%, respectively. Compared with the AIEgen monomer **EM**, copolymer **P(NIPAM-*co*-EM)** shows the specific AIEE activity since its AIE-active luminogen can be enhanced by the polymer chain of **PNIPAM**. It is reasonable that the polymer matrix of **PNIPAM** can restrict the exciton energy consumption to a certain extent from the rotation and vibration of the grafted AIEgen monomer **EM**.

Thermo-responsive behavior of P(NIPAM-*co*-EM)

The LCST can be usually modified by hydrophobic or hydrophilic monomers/crosslinking agents.[53] Considering both the

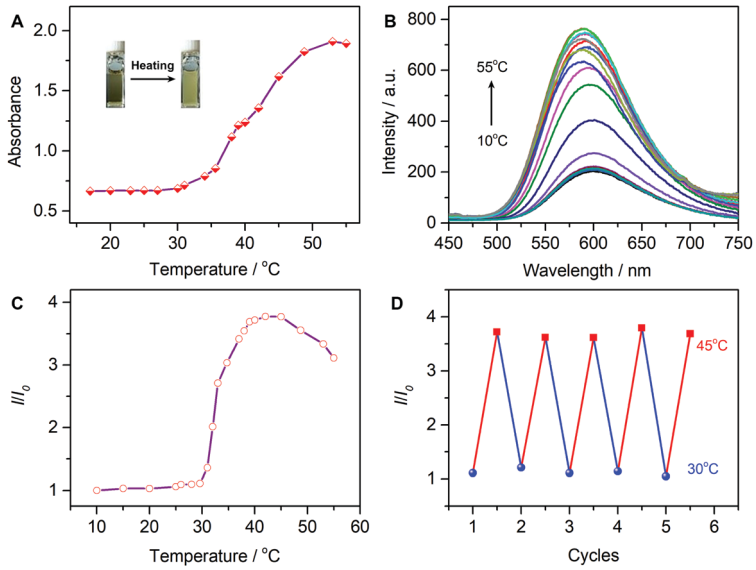

Fig. 5 LCST-featured behavior: (A) temperature-dependent absorption at 430 nm of **P(NIPAM-*co*-EM)** (14 μM) in an aqueous solution upon heating; inset: images of **P(NIPAM-*co*-EM)** before and after heating. (B) Temperature-dependent emission spectra of **P(NIPAM-*co*-EM)** (14 μM), λ_{ex} = 430 nm. (C) The relative fluorescent intensity at 607 nm as a function of temperature. (D) Reversible thermo-response of **P(NIPAM-*co*-EM)** between 30 and 45 °C by monitoring the fluorescent signal.

hydrophobicity and temperature sensitivity, we copolymerized the monomers of **NIPAM** and AIEgen **EM** into the LCST-featuring **P(NIPAM-*co*-EM)**. Here, the copolymer **P(NIPAM-*co*-EM)** would form coil micelles in water below the LCST. When heating to a temperature above the LCST, the originally extended hydrophilic polymer chains would change into an entangled hydrophobic globule state. The dehydration process upon heating can lead to the formation of tight nanoparticles, causing turbidity in the polymer aqueous solution. As shown in Fig. 5A, upon increasing the temperature, the absorbance showed almost no change below the LCST temperature. In contrast, when the temperature was approaching the LCST point (around 30 °C), the absorbance started to increase continuously until 55 °C. The solution change from clear to turbid indicated that the system transformed from a hydrophilic state to hydrophobic state due to the solubility loss on heating. Moreover, the copolymer upon cooling showed a reversible process (Fig. S5, ESI†), indicative of a clear LCST temperature. Obviously, the LCST-featuring copolymer **P(NIPAM-*co*-EM)** can undergo a transition from coil to globule state in an aqueous solution.

The fluorescence behavior of the thermometer was also examined upon heating (Fig. 5B). Accompanying the increase in temperature, the luminescence intensity showed only a negligible increase below the LCST (30 °C). When heating to the temperature above 30 °C, a sharp luminescence increase between 30–45 °C was observed with a fluorescence enhancement of about 3.7-fold (Fig. 5C). However, the continuous heating above 45 °C caused a fluorescence decrease due to the active thermal motion with relaxing the excited state. Also, the fluorescence peak showed a small blue-shift of 10 nm upon continuous heating, which might have resulted from the less polar microenvironment formed from the dehydration process.

The AIEgen-grafted copolymer can be potentially developed as a fluorescent thermometer through its AIEE mechanism. That is, we explored the AIEgen-grafted copolymer **P(NIPAM-*co*-EM)** with a thermo-responsive polymer **PNIPAM** as a LCST matrix for constructing an AIE fluorescent thermometer. As depicted in Fig. 5D, the temperature repeatability and reversibility were well dependent upon the copolymer emission in the range from 30 to 45 °C, corresponding to the specific LCST feature from **PNIPAM**. Based on the precise modulation and excellent consistency, the temperature effect on the LCST-featured microstructure of the **PNIPAM** chain can disturb the AIEgen aggregation behavior, thereby achieving a specific AIE-active fluorescent thermometer.

Conclusions

Enlightened by the unique AIE properties, we explored the AIEgen-grafted copolymer **P(NIPAM-*co*-EM)** with a thermo-responsive polymer **PNIPAM** as a LCST-featuring matrix for developing an AIE fluorescent thermometer. The polymer **P(NIPAM-*co*-EM)** with LCST transition underwent a characteristic transition from coil to globule state in aqueous solution due to the solubility loss on heating. Based on the specific LCST behavior of **PNIPAM**, the temperature response was well consistent with the copolymer emission with good repeatability and reversibility in the range from 30 to 45 °C, where the temperature effect on the LCST-featuring microstructure of the **PNIPAM** chain can disturb the AIEgen aggregation behavior, thereby achieving a specific AIE-active fluorescent thermometer. Based on the precise modulation and excellent consistency, the AIEgen-grafted copolymer system can be potentially used as fluorescence-enhanced thermometer

through its AIEE mechanism, which might overcome the traditional problem of thermal-induced fluorescence quenching.

Conflicts of interest

There are no conflicts to declare.

Acknowledgements

This work was supported by the NSFC Science Center Program (21788102) and Creative Research Groups (21421004), the National Key Research and Development Program (2016YFA0200300 and 2017YFC0906902), NSFC/China (21636002, 21622602, and 21607044), the Shanghai Municipal Science and Technology Major Project (2018SHZDZX03), the National Postdoctoral Program for Innovative Talents (BX201700075), the Program of Introducing Talents of Discipline to Universities (B16017), and the Natural Science Foundation of Hebei Province (B2017502069).

Notes and references

1 H. Liu, L. Chen, C. Xu, Z. Li, H. Zhang, X. Zhang and W. Tan, *Chem. Soc. Rev.*, 2018, **47**, 7140–7180.
2 D. Wu, A. C. Sedgwick, T. Gunnlaugsson, E. U. Akkaya, J. Yoon and T. D. James, *Chem. Soc. Rev.*, 2017, **46**, 7105–7123.
3 K. Gu, W. H. Zhu and X. Peng, *Sci. China: Chem.*, 2019, **62**, 189–198.
4 M. H. Lee, J. S. Kim and J. L. Sessler, *Chem. Soc. Rev.*, 2015, **44**, 4185–4191.
5 Y. Wu, S. Huang, J. Wang, L. Sun, F. Zeng and S. Wu, *Nat. Commun.*, 2018, **9**, 3983.
6 A. C. Sedgwick, W. Dou, J. Jiao, L. Wu, G. T. Williams, A. T. A. Jenkins, S. D. Bull, J. L. Sessler, X. He and T. D. James, *J. Am. Chem. Soc.*, 2018, **140**, 14267–14271.
7 D. Yue, M. Wang, F. Deng, W. Yin, H. Zhao, X. Zhao and Z. Xu, *Chin. Chem. Lett.*, 2018, **29**, 648–656.
8 X. Zhou, Y. Zeng, C. Liyan, X. Wu and J. Yoon, *Angew. Chem., Int. Ed.*, 2016, **55**, 4729–4733.
9 H. Li, Y. Li, Q. Yao, J. Fan, W. Sun, S. Long, K. Shao, J. Du, J. Wang and X. Peng, *Chem. Sci.*, 2019, **10**, 1619–1625.
10 X. Zhang, Y. Yan, Q. Peng, J. Wang, Y. Hang and J. Hua, *Mater. Chem. Front.*, 2017, **1**, 2292–2298.
11 Y. Qi, Y. Huang, B. Li, F. Zeng and S. Wu, *Anal. Chem.*, 2017, **90**, 1014–1020.
12 Y. Li, Y. Sun, J. Li, Q. Su, W. Yuan, Y. Dai, C. Han, Q. Wang, W. Feng and F. Li, *J. Am. Chem. Soc.*, 2015, **137**, 6407–6416.
13 J. Luo, Z. Xie, J. W. Y. Lam, L. Cheng, H. Chen, C. Qiu, H. S. Kwok, X. Zhan, Y. Liu, D. Zhu and B. Z. Tang, *Chem. Commun.*, 2001, 1740–1741.
14 Y. Hong, J. W. Y. Lam and B. Z. Tang, *Chem. Commun.*, 2009, 4332–4353.
15 J. Mei, N. L. C. Leung, R. T. K. Kwok, J. W. Y. Lam and B. Z. Tang, *Chem. Rev.*, 2015, **115**, 11718–11940.
16 Z. Zhao, C. Chen, W. Wu, F. Wang, L. Du, X. Zhang, Y. Xiong, X. He, Y. Cai, R. T. K. Kwok, J. W. Y. Lam, X. Gao, P. Sun, D. L. Phillips, D. Ding and B. Z. Tang, *Nat. Commun.*, 2019, **10**, 768.
17 S. Zhen, S. Wang, S. Li, W. Luo, M. Gao, L. G. Ng, C. C. Goh, A. Qin, Z. Zhao, B. Liu and B. Z. Tang, *Adv. Funct. Mater.*, 2018, **28**, 1706945.
18 R. T. K. Kwok, C. W. T. Leung, J. W. Y. Lam and B. Z. Tang, *Chem. Soc. Rev.*, 2015, **44**, 4228–4238.
19 K. C. Chong, F. Hu and B. Liu, *Mater. Chem. Front.*, 2019, **3**, 12–24.
20 H. Gao, X. Zhang, C. Chen, K. Li and D. Ding, *Adv. Biosyst.*, 2018, **2**, 1800074.
21 Z. Guo, A. Shao and W. H. Zhu, *J. Mater. Chem. C*, 2016, **4**, 2640–2646.
22 D. Li and J. Yu, *Small*, 2016, **12**, 6478–6494.
23 A. Nicol, R. T. K. Kwok, C. Chen, W. Zhao, M. Chen, J. Qu and B. Z. Tang, *J. Am. Chem. Soc.*, 2017, **139**, 14792–14799.
24 J. Yang, Z. Ren, Z. Xie, Y. Liu, C. Wang, Y. Xie, Q. Peng, B. Xu, W. Tian, F. Zhang, Z. Chi, Q. Li and Z. Li, *Angew. Chem., Int. Ed.*, 2017, **56**, 880–884.
25 M. Gao, S. Li, Y. Lin, Y. Geng, X. Ling, L. Wang, A. Qin and B. Z. Tang, *ACS Sens.*, 2016, **1**, 179–184.
26 S. Uchiyama, T. Tsuji, K. Kawamoto, K. Okano, E. Fukatsu, T. Noro, K. Ikado, S. Yamada, Y. Shibata, T. Hayashi, N. Inada, M. Kato, H. Koizumi and H. Tokuyama, *Angew. Chem., Int. Ed.*, 2018, **57**, 5413–5417.
27 K. Okabe, N. Inada, C. Gota, Y. Harada, T. Funatsu and S. Uchiyama, *Nat. Commun.*, 2012, **3**, 705.
28 Y. Takei, S. Arai, A. Murata, M. Takabayashi, K. Oyama, S. I. Ishiwata, S. Takeoka and M. Suzuki, *ACS Nano*, 2014, **8**, 198–206.
29 J. Feng, K. Tian, D. Hu, S. Wang, S. Li, Y. Zeng, Y. Li and G. Yang, *Angew. Chem., Int. Ed.*, 2011, **50**, 8072–8076.
30 L. Tang, J. K. Jin, A. Qin, W. Zhang Yuan, Y. Mao, J. Mei, J. Zhi Sun and B. Z. Tang, *Chem. Commun.*, 2009, 4974–4976.
31 J. Qiao, C. Chen, D. Shangguan, X. Mu, S. Wang, L. Jiang and L. Qi, *Anal. Chem.*, 2018, **90**, 12553–12558.
32 C. Wang, W. Huang and J. Liao, *J. Phys. Chem. B*, 2015, **119**, 3720–3726.
33 R. Plummer, D. J. T. Hill and A. K. Whittaker, *Macromolecules*, 2006, **39**, 8379–8388.
34 S. Backes, P. Krause, W. Tabaka, M. U. Witt, D. Mukherji, K. Kremer and R. von Klitzing, *ACS Macro Lett.*, 2017, **6**, 1042–1046.
35 X. Lang, W. R. Lenart, J. E. P. Sun, B. Hammouda and M. J. A. Hore, *Macromolecules*, 2017, **50**, 2145–2154.
36 S. Uchiyama, Y. Matsumura, A. P. de Silva and K. Iwai, *Anal. Chem.*, 2004, **76**, 1793–1798.
37 D. Wang, R. Miyamoto, Y. Shiraishi and T. Hirai, *Langmuir*, 2009, **25**, 13176–13182.
38 Z. Guo, W. Zhu, Y. Xiong and H. Tian, *Macromolecules*, 2009, **42**, 1448–1453.
39 C. Chen and C. Chen, *Chem. Commun.*, 2011, **47**, 994–996.
40 J. B. Birks, *Photophysics of Aromatic Molecules*, Wiley, London, 1970.

41 M. R. Shreykar and N. Sekar, *J. Fluoresc.*, 2017, **27**, 1687–1707.
42 B. An, J. Gierschner and S. Y. Park, *Acc. Chem. Res.*, 2012, **45**, 544–554.
43 J. Mei, Y. Huang and H. Tian, *ACS Appl. Mater. Interfaces*, 2018, **10**, 12217–12261.
44 W. Wu, D. Mao, S. Xu, S. Ji, F. Hu, D. Ding, D. Kong and B. Liu, *Mater. Horiz.*, 2017, **4**, 1110–1114.
45 Z. Guo, W. H. Zhu and H. Tian, *Chem. Commun.*, 2012, **48**, 6073–6084.
46 K. Gu, Y. Xu, H. Li, Z. Guo, S. Zhu, S. Zhu, P. Shi, T. D. James, H. Tian and W. H. Zhu, *J. Am. Chem. Soc.*, 2016, **138**, 5334–5340.
47 W. Fu, C. Yan, Z. Guo, J. Zhang, H. Zhang, H. Tian and W. H. Zhu, *J. Am. Chem. Soc.*, 2019, **141**, 3171–3177.
48 K. Gu, W. Qiu, Z. Guo, C. Yan, S. Zhu, D. Yao, P. Shi, H. Tian and W. H. Zhu, *Chem. Sci.*, 2019, **10**, 398–405.
49 Y. Li, A. Shao, Y. Wang, J. Mei, D. Niu, J. Gu, P. Shi, W. H. Zhu, H. Tian and J. Shi, *Adv. Mater.*, 2016, **28**, 3187–3193.
50 A. Shao, Y. Xie, S. Zhu, Z. Guo, S. Zhu, J. Guo, P. Shi, T. D. James, H. Tian and W. H. Zhu, *Angew. Chem., Int. Ed.*, 2015, **54**, 7275–7280.
51 A. Shao, Z. Guo, S. Zhu, S. Zhu, P. Shi, H. Tian and W. H. Zhu, *Chem. Sci.*, 2014, **5**, 1383–1389.
52 C. Shi, Z. Guo, Y. Yan, S. Zhu, Y. Xie, Y. S. Zhao, W. H. Zhu and H. Tian, *ACS Appl. Mater. Interfaces*, 2013, **5**, 192–198.
53 H. Feil, Y. H. Bae, J. Feijen and S. W. Kim, *Macromolecules*, 1993, **26**, 2496–2500.